Lunar Dust Migration by Electrostatic Charging: Numerical Modelling J.-C. Matéo-Vélez[1], P. Sarrailh[1], S. L. G. Hess[1], B. Jeanty-Ruard[2], F. Cipriani[3], S. R. Marple[4], B. Thiébault[2], J. Forest[2] and F. Honary[4], [1]ONERA, BP74025, 2 avenue Edouard Belin, FR-31055 Toulouse, France (mateo@onera.fr), [2]ARTENUM, 24 rue Louis Blanc, FR-75010 Paris, France (j.forest@artenum.com), [3]ESA/ESTEC TEC-MMG, Keplerlaan 1, 2200AG Noordwijk ZH, The Netherlands, [4]Lancaster University, Department of Physics, Lancaster, UK

Introduction: Since the Apollo era dust contamination is clearly an identified risk for space objects exploration missions. The lunar Horizon Glow is believed to occur at the transition of sunlit and shaded surfaces due to the combination of charged dust and large electric field [1]-[2]. Human or robotic activities also remove dust from the soil with possible subsequent adhesion onto sensitive surfaces, by a combination of forces acting on them, including gravity and electromagnetic. Recent pictures of the Rosetta mission suggested a large amount of volatile small dusts kicked up by Philae rebounds on the comet soil. Identifying the process leading to dust adhesion onto surfaces is a key aspect of space exploration. One of the main contributors is the electrostatic charging imposed by the space environment. This paper aims to describe the numerical tool developed under ESA contract #4000107327 modelling the physics at the origin of lunar dust migration by electrostatic means and subsequent contamination.

Overview of the approach: it includes the detailed description of the objects (lunar soil, lander geometry, dust properties) as well as the coupling with the ambient plasma conditions. The complex system interconnections include physics of lunar soil charging, forces acting on dust, dynamics in the gaseous phase and finally Lander/Rover contamination. The Lander itself plays a role on dust transport. The open-source Spacecraft Plasma Interaction Software (SPIS) is used and further developed to handle this multi physics and multi scales problem.

Lunar dust and Lander geometry: Charging occurs at different length scales (the lunar surface, dusts and the lander) and different time scales (electron, proton, dust dynamics).

Lunar surface geometry: The Lunar or asteroid surface is modelled either in two or three dimensions with detailed shapes such as craters. (X,Y,Z) Cartesian coordinates of the surface are possible to set with text files.

Lander definition: The lander is built in an independent file defining the dimensions and groups of similar materials. It is then merged with the lunar surface mesh to obtain a set of material boundaries for the volume plasma computation.

Computational domain: The length of the simulated domain is about some tens or hundreds of Debye lengths in 2D and some Debye lengths in 3D, only limited by the computational time and memory constraints. On one side, the boundary conditions imposed on the lunar and Lander are Dirichlet potentials. On the other side, it consists in symmetry and periodic conditions for both matter and fields.

Lunar dust properties: The lunar regolith is composed of basalt in the lunar seas and feldspar rocks in the Highlands. The distribution of interest in this work is typically dust below 100 µm in diameter, composed of silica, ferrite, alumina and other components, with a global density of 1.5 g/cm^3. Reviews of Apollo missions' data are used to set the dust distributions [3].

Electron emission: The photoemission process depends on the sun flux and energy distribution as well as the material properties and surface state. The secondary electron emission (SEE) is important to determine the potentials of shaded dust and soil. The SEE yield is a combination of primary electron energy, incidence angle and material properties. The models implemented account for dust surface layer as well as isolated dusts [4].

Conductivity: shaded dusts are considered as very resistive. Sunlit dusts are very conductive [3]. It impacts the differential charging at the origin of strong electric fields at sun/shade transition regions.

Plasma sheath: The important parameters for plasma interaction with the lunar/asteroid surface are the distance to the Sun and the presence of a magnetosphere, defining the ambient electron and proton distributions. On the dayside, the main contributor to soil and dust charging is the photoemission. The surface floats to a few volts positive. On the night side or in shade, the ambient plasma makes the surface potential float to some tens or hundreds of volts negative. The important parameter there is the SEE yield of the lunar soil. In between, the terminator is a region of increasing electric field, especially when taking into account the surface roughness and craters [4]. The plasma sheath model accounts for the impact of photoelectrons on the plasma quasi neutrality condition. The electric field is computed by solving the Poisson equation. A dipole-like magnetic field accounts for crustal fields.

The Particle-In-Cell model agrees previous results in a large range of solar zenith angles (SZA) [5].

Dust migration: Two mechanisms of dust release are considered: electrostatics and mechanics.

Electrostatic release: The charging of dust is computed by solving the Gauss equation at the lunar surface. Dust ejection is performed when the electrostatic force balances the gravity and adhesion forces.

Seismic or Human activity: this extra source of dust ejection is modeled by user defined dust distributions in radius and velocity.

Lander contamination: Released dusts continue to charge in the gaseous phase and are accelerated by the electromagnetic fields imposed by the plasma and by the objects. The surface potential on-board takes account of the material properties in terms of electron emission and conduction. A typical configuration consists in shaded dielectrics that may float negatively with respect to the spacecraft ground and collect positively charged dust. The dust hazard (obscuration, abrasion) is a key output of the tool which uses the key parameters defined by [7].

Applications to the lunar surface: The next figure represents a typical map of dust average radius (log scale) above a sunlit flat lunar surface at SZA = 0°. In this simulation the dust mean radius is about some (tens of) nanometers at a distance of 40 m. The complex potential structure generated by a small crater and a lander on the Moon is given in the following figure. The view consists in the surface potential and a perpendicular cut of the volume potential. The SZA of 45° makes the crater charge differentially, generating dust levitation and adhesion onto lander surfaces (located on the right of the crater). Further results have been obtained in the following configurations:

Asteroid Surface: A 2D geometry was built to represent a tentative surface of the asteroid Bennu (101955) 1999 RQ36, including craters at different SZA.

Ground experiment: Finally, experiments presented in a companion abstract will be modeled. The observed displacement of lunar dust simulants induced by VUV charging and polarized surfaces can be reproduced at least qualitatively by the model. It permits to optimize the test setup.

Perspectives: This study presents efforts conducted under ESA contract #4000107327 to numerically model dust electrostatic charging and contamination, mimicking what is expected during Moon and asteroids exploration missions. The SPIS-Dust tool has been applied to a variety of cases and is a solution for estimating dust contamination risks and for designing mitigation techniques, as a complement to ground testing. The genericity of the model will enable to add physical modules (as *e.g.* micrometeorite impact, large scale simulations) and upgrade detailed models for dust interactions.

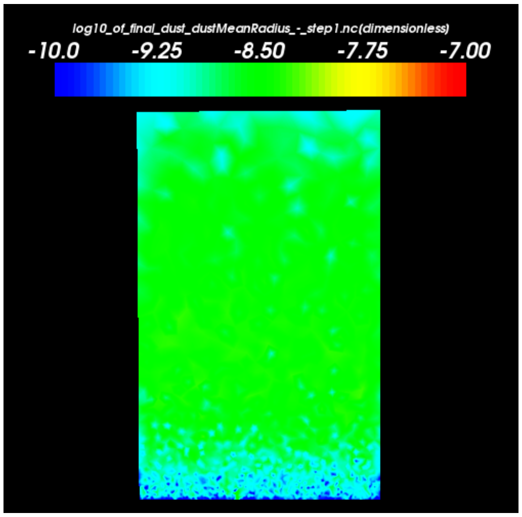

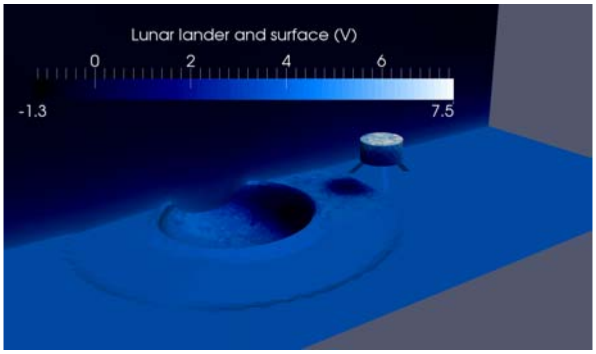

References: [1] Criswell D. R. (1973), Photon and Particle Interactions with Surfaces in Space, 545-556. [2] Rennilson J., Criswell D. R. (1974), The Moon, 121-142. [3] Heiken G. H., Lunar sourcebook (1991), 307 and 531. [4] Chow, V. W. et al (1993), JGR, 98(A11), 19065-19076. [5] Poppe, A., et al. (2012), Icarus, 221, 135-146. [6] Poppe, A. and Horanyi, M. (2010), JGR, 115, A08106. [7] Kobrick, R. L., et al (2011), Planetary and Space Science, 59, 1749–1757. [8] Hess, S., et al. (2014), 13th SCTC proc.